ISSN 1070-3284, Russian Journal of Coordination Chemistry, 2019, Vol. 45, No. 3, pp. 222–229. © Pleiades Publishing, Ltd., 2019.

Two *cis*-Dioxomolybdenum(VI) Complexes with Tridentate ONO Aroylhydrazone Schiff Bases: Syntheses, Characterization, Crystal Structures, and Catalytic Epoxidation Property[1]

Y. M. Cui[a, b], W. T. Liu[a, c], and W. X. Yan[d, *]

[a] *Engineering Research Center for Clean Production of Textile Printing and Dyeing, Ministry of Education, Wuhan Textile University, Wuhan, 430073 P.R. China*

[b] *School of Environmental Engineering, Wuhan Textile University, Wuhan, 430073 P.R. China*

[c] *China Meheco Liyi Pharm Sci and Tech Co., Ltd., Wuhan, 430073 P.R. China*

[d] *Library of Wuhan Textile University, Wuhan, 430073 P.R. China*

**e-mail: cuiym981248@163.com*

Received April 29, 2018; revised June 27, 2018; accepted October 20, 2018

Abstract—Two new *cis*-dioxomolybdenum(VI) complexes, $[MoO_2(L^1)MeOH]$ (**I**) and $[MoO_2(L^2)MeOH]$ (**II**) with potentially tridentate ONO aroylhydrazone Schiff bases derived from 3-methoxysalicylaldehyde with 4-bromobenzohydrazide and 4-trifluoromethylbenzohydrazide, respectively, have been synthesized and fully characterized on the basis of elemental analysis, FT-IR, molar conductivity, and electronic spectra. Structures of the complexes have been accomplished by single crystal X-ray diffraction (CIF files CCDC nos. 1433352 (**I**) and 1433318 (**II**)). The complexes have distorted octahedral structures in which the aroylhydrazones behave as binegative ligands. It is also revealed from the crystal structures that the Mo(VI) center adopts NO_5 donor environment, and the octahedral coordination is furnished by two oxido groups and oxygen atoms of methanol or deprotonated methanol molecules. The catalytic properties were investigated for epoxidation of cyclooctene using aqueous *tert*-butyl hydroperoxide as the oxidant.

Keywords: dioxomolybdenum(VI) complexes, froylhydrazone, Schiff base, X-ray crystal structure, catalytic epoxidation property

DOI: 10.1134/S1070328419030023

INTRODUCTION

In recent years, Schiff base ligands and their transition metal complexes have attracted considerable attention, not only for their facile synthesis, but also for potential biological, catalytic and industrial applications [1–5]. As we know, catalytic epoxidation of olefins is an important reaction in organic synthesis. Many transition metal complexes are active catalysts for this process [6–10]. Yet, among the complexes, molybdenum complexes have a unique place in coordination chemistry and have displayed very high catalytic activities in the oxidation of olefins and sulfides [11–13]. To date, the relationship between structures and catalytic epoxidation activity of the molybdenum complexes is still less studied. In the present work, two similar aroylhydrazone Schiff bases, 4-bromo-(*N*′-2-hydroxy-3-methoxybenzylidene)benzohydrazide (H_2L^1) and *N*′-(2-hydroxy-3-methoxybenzylidene)-4-trifluoromethylbenzohydrazide (H_2L^2) with different terminal substitute groups, were prepared and used to prepare dioxomolybdemum(VI) complexes with $MoO_2(Acac)_2$ in methanol. The catalytic properties were investigated for epoxidation of cyclooctene using aqueous *tert*-butyl hydroperoxide as the oxidant.

[1] The article is published in the original.

EXPERIMENTAL

Materials and methods. 4-Bromobenzohydrazide and 4-trifluoromethylbenzohydrazide were prepared as described in the literature [14]. 3-Methoxysalicylaldehyde was purchased from Alfa Aesar and used as received. $MoO_2(Acac)_2$ was prepared as described in the literature [15]. Reagent grade solvents were used as received. Microanalyses of the complexes were performed with a Vario EL III CHNOS elemental analyzer. Infrared spectra were recorded as KBr pellets with an FTS-40 spectrophotometer. Electronic spectra were recorded on a Lambda 900 spectrometer. ^1H NMR spectra were recorded on a 500 MHz Bruker Advance instrument. The catalytic reactions were followed by gas chromatography on an Agilent 6890A chromatograph equipped with an FID detector and a DB5-MS capillary column (30 m × 0.32 mm × 0.25 μm). Molar conductance measurements were

made by means of a Metrohm 712 conductometer in acetonitrile.

Synthesis of the aroylhydrazone Schiff bases H_2L^1 and H_2L^2 was carried out in a similar way by refluxing a methanolic solution (30 mL) of 3-methoxysalicylaldehyde (10 mmol, 1.52 g) with 4-bromobenzohydrazide (10 mmol, 2.15 g) and 4-trifluoromethylbenzohydrazide (10 mmol, 2.04 g), respectively. Reflux was continued for 1 h at oily bath during which a solid compound separated. It was filtered and washed with cold methanol. The crude product was recrystallized from methanol and dried over anhydrous $CaCl_2$.

H_2L^1: yield was 2.89 g (83%). IR data (KBr pellet; ν, cm^{-1}): 3384 ν(O–H), 3233 ν(N–H), 1653 ν(C=O), 1610 ν(C=N). UV-Vis data (methanol; λ, nm): 290, 355, 410. ^{1}H NMR (300 MHz; DMSO; δ, ppm): 12.13 (s., 1H, N*H*), 9.73 (s., 1H, O*H*), 8.91 (s., 1H, C*H*=N), 8.15 (d., 2H, Ar*H*), 7.87 (d., 2H, Ar*H*), 7.31 (d., 1H, Ar*H*), 7.22 (d., 1H, Ar*H*), 7.01 (t., 1H, Ar*H*), 3.82 (s., 3H, OCH_3).

For $C_{15}H_{13}N_2O_3Br$

Anal. calcd., %	C, 51.60	H, 3.75	N, 8.02
Found, %	C, 51.77	H, 3.83	N, 7.96

H_2L^2: yield was 3.03 g (90%). IR data (KBr pellet; ν, cm^{-1}): 3405 ν(O–H), 3226 ν(N–H), 1649 ν(C=O), 1613 ν(C=N). UV-Vis data (methanol; λ, nm): 295, 360, 418. ^{1}H NMR (300 MHz; DMSO; δ, ppm): 12.21 (s., 1H, N*H*), 9.82 (s., 1H, O*H*), 8.90 (s., 1H, C*H*=N), 7.91 (d., 2H, Ar*H*), 7.76 (d., 2H, Ar*H*), 7.31 (d., 1H, Ar*H*), 7.17 (d., 1H, Ar*H*), 6.96 (t., 1H, Ar*H*), 3.80 (s., 3H, OCH_3).

For $C_{16}H_{13}N_2O_3F_3$

Anal. calcd., %	C, 56.81	H, 3.87	N, 8.28
Found, %	C, 56.63	H, 3.96	N, 8.37

Synthesis of $[MoO_2(L^1)MeOH]$ (I) and $[MoO_2(L^2)MeOH]$ (II). The complexes **I** and **II** were prepared in a similar way by refluxing a methanolic solution (30 mL) of $MoO_2(Acac)_2$ (1.0 mmol, 0.33 g) with methanolic solutions of H_2L^1 (1.0 mmol, 0.35 g) and H_2L^2 (1.0 mmol, 0.34 g), respectively. Initially on mixing the two components immediately an orange yellow color was observed. The mixture was refluxed for 1 h. The respective complex separated as orange single crystals during slow evaporation of the reaction mixture. It was filtered, washed with cold methanol and dried over anhydrous $CaCl_2$.

I: yield was 0.31 g (61%). IR data (KBr pellet; ν, cm^{-1}): 3446 ν(O–H), 1605 ν(C=N), 1358 ν(C–$O_{phenolate}$), 1157 ν(N–N), 950 ν_{sym}(*cis*-MoO_2), 861 ν_{asym}(*cis*-MoO_2). UV-Vis data (acetonitrile; λ, nm): 295, 430. ^{1}H NMR (300 MHz; DMSO; δ, ppm): 9.00 (s., 1H, C*H*=N), 8.20 (d., 2H, Ar*H*), 7.90 (d., 2H, Ar*H*), 7.35 (d., 1H, Ar*H*), 7.27 (d., 1H, Ar*H*), 7.05 (t., 1H, Ar*H*), 4.10 (q., 3H, CH_3OH), 3.82 (s., 3H, OCH_3). Molar conductance (10^{-3} M, acetonitrile): 27 Ω^{-1} cm^2 mol^{-1}.

For $C_{16}H_{15}N_2O_6BrMo$

Anal. calcd., %	C, 37.89	H, 2.98	N, 5.52
Found, %	C, 37.70	H, 3.12	N, 5.66

II: yield was 0.37 g (75%). IR data (KBr pellet; ν, cm^{-1}): 3453 ν(O–H), 1607 ν(C=N), 1383 ν(C–$O_{phenolate}$), 1157 ν(N–N), 950 ν_{sym}(*cis*-MoO_2), 850 ν_{asym}(*cis*-MoO_2). ^{1}H NMR (300 MHz; DMSO; δ, ppm): 8.92 (s., 1H, C*H*=N), 7.90 (d., 2H, Ar*H*), 7.72 (d., 2H, Ar*H*), 7.31 (d., 1H, Ar*H*), 7.26 (d., 1H, Ar*H*), 7.02 (t., 1H, Ar*H*), 4.08 (q., 3H, CH_3OH), 3.80 (s., 3H, OCH_3). UV-Vis data (acetonitrile; λ, nm): 300, 430. Molar conductance (10^{-3} M, acetonitrile): 32 Ω^{-1} cm^2 mol^{-1}.

For $C_{17}H_{15}N_2O_6F_3Mo$

Anal. calcd., %	C, 41.15	H, 3.05	N, 5.65
Found, %	C, 41.31	H, 3.14	N, 5.53

X-ray structure determination. Data were collected on a Bruker SMART 1000 CCD area diffractometer using a graphite monochromator MoK_α radiation (λ = 0.71073 Å) at 298(2) K. The data were corrected with SADABS programs and refined on F^2 with Siemens SHELXL software [16, 17]. The structures were solved by direct methods and difference Fourier syntheses. All non-hydrogen atoms were refined anisotropically. The methanol hydrogen atoms were located from difference Fourier maps and refined isotropically, with O–H distances restrained to 0.85(1) Å. The remaining hydrogen atoms were placed in calculated positions and included in the last cycles of refinement. Crystal data and details of the data collection and refinement are listed in Table 1. Selected coordinate bond lengths and angles are listed in Table 2.

Supplementary material for structures has been deposited with the Cambridge Crystallographic Data Centre (CCDC nos. 1433352 (**I**) and 1433318 (**II**); deposit@ccdc.cam.ac.uk or http://www.ccdc.cam.ac.uk).

Catalytic epoxidation process. A mixture of cyclooctene (2.76 mL, 20 mmol), acetophenone (internal reference) and the complexes as catalysts (0.05 mmol) was stirred and heated up to 80°C before addition of aqueous *tert*-butyl hydroperoxide (TBHP; 70% w/w, 5.48 mL, 40 mmol). The mixture is initially an emulsion, but two phases become clearly visible as the reaction progresses, a colorless aqueous one and a yellowish organic one. The reaction was monitored for 5 h with withdrawal and analysis of organic phase ali-

Table 1. Crystallographic data and structure refinement for complexes for **I** and **II**

Parameters	Value	
	I	**II**
Formula weight	507.15	496.25
Crystal system	Monoclinic	Monoclinic
Space group	$P2_1/c$	$P2_1/c$
a, Å	13.061(1)	13.8574(9)
b, Å	10.1521(5)	10.4350(5)
c, Å	14.639(1)	14.663(1)
β, deg	110.292(2)	114.427(2)
V, Å^3	1820.6(2)	1930.5(2)
Z	4	4
ρ_{calcd}, g cm^{-3}	1.850	1.707
μ, mm^{-1}	2.950	0.745
F(000)	1000	992
θ Range for data collection	2.85–25.50	3.05–25.50
Index ranges	$-15 \le h \le 11$, $-12 \le k \le 12$, $-17 \le l \le 17$	$-16 \le h \le 14$, $-10 \le k \le 12$, $-13 \le l \le 17$
Measured reflections	7901	9542
Independent reflections	3383	3585
Observed reflections ($I > 2\sigma(I)$)	2582	2919
Parameters	240	267
Restraints	1	1
Data completeness	0.999	0.999
T_{max}/T_{min}	0.4715/0.5259	0.8533/0.8654
Final R indices ($I > 2\sigma(I)$)	0.0353, 0.0727	0.0372, 0.0949
R indices (all data)	0.0548, 0.0809	0.0494, 0.1042
Goodness-of-fit on F^2	1.023	1.064
Largest difference in peak and hole, e Å^{-3}	0.452 and –0.651	0.885 and –0.550

Table 2. Selected bond lengths (Å) and angles (deg) for the complexes

Bond	*d*, Å	Bond	*d*, Å
		I	
Mo(1)–O(1)	1.916(2)	Mo(1)–O(2)	2.017(2)
Mo(1)–O(4)	1.691(2)	Mo(1)–O(5)	1.692(2)
Mo(1)–O(6)	2.348(3)	Mo(1)–N(1)	2.244(3)
		II	
Mo(1)–O(1)	1.912(2)	Mo(1)–O(2)	2.012(2)
Mo(1)–O(4)	1.698(3)	Mo(1)–O(5)	1.695(2)
Mo(1)–O(6)	2.359(3)	Mo(1)–N(1)	2.246(3)
Angle	ω, deg	Angle	ω, deg
		I	
O(1)Mo(1)O(2)	148.18(9)	O(1)Mo(1)N(1)	80.65(10)
O(4)Mo(1)O(1)	100.03(11)	O(4)Mo(1)O(2)	96.73(12)
O(4)Mo(1)O(5)	105.40(12)	O(4)Mo(1)N(1)	94.05(11)
O(5)Mo(1)O(1)	103.63(12)	O(5)Mo(1)O(2)	97.66(11)
O(5)Mo(1)N(1)	158.81(11)	O(2)Mo(1)N(1)	71.31(9)
O(4)Mo(1)O(6)	171.72(12)	O(5)Mo(1)O(6)	81.94(11)
O(1)Mo(1)O(6)	81.62(10)	O(2)Mo(1)O(6)	78.23(10)
N(1)Mo(1)O(6)	78.15(10)		
		II	
O(1)Mo(1)O(2)	149.30(10)	O(1)Mo(1)N(1)	81.04(9)
O(4)Mo(1)O(1)	100.35(12)	O(4)Mo(1)O(2)	95.41(12)
O(5)Mo(1)O(1)	103.00(11)	O(5)Mo(1)O(2)	97.70(11)
O(5)Mo(1)O(4)	105.90(14)	O(5)Mo(1)N(1)	157.01(13)
O(4)Mo(1)N(1)	95.41(12)	O(2)Mo(1)N(1)	71.33(9)
O(5)Mo(1)O(6)	82.91(12)	O(4)Mo(1)O(6)	170.05(11)
O(1)Mo(1)O(6)	81.74(10)	O(2)Mo(1)O(6)	78.56(10)
N(1)Mo(1)O(6)	75.22(9)		

quots (0.1 mL) at required times. Each withdrawn sample was mixed with 2 mL of diethylether, treated with a small quantity of MnO_2 and then filtered through silica and analyzed by GC.

RESULTS AND DISCUSSION

The aroylhydrazone Schiff bases and their complexes were synthesized in a facile and essentially identical way (Scheme 1).

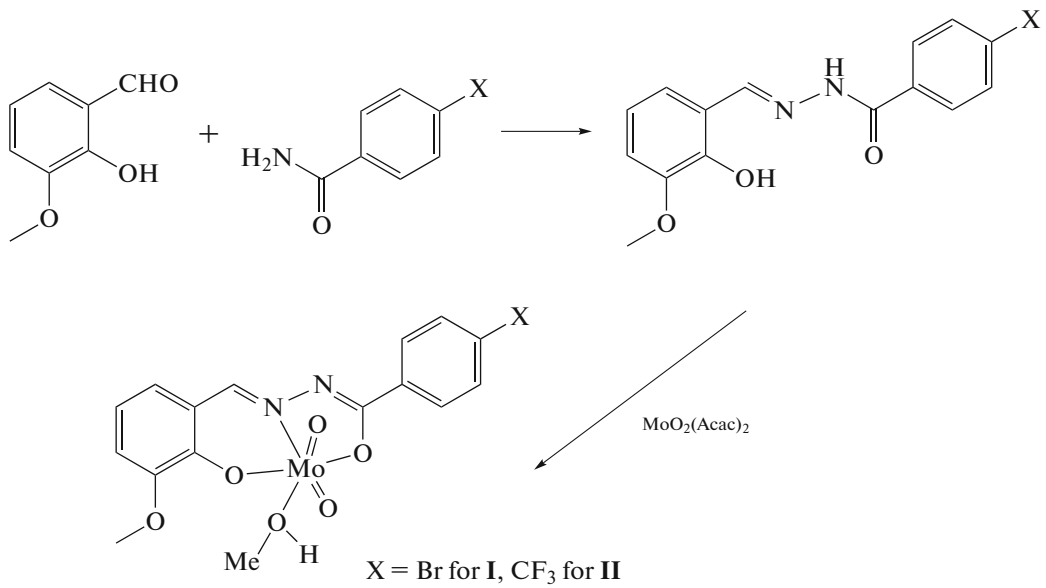

Scheme 1.

The aroylhydrazone Schiff bases act as tridentate dianionic ONO donor ligands toward the MoO_2^{2+} core. Both Mo(VI) complexes were obtained from a refluxing mixture of the respective ligand and $MoO_2(Acac)_2$ in 1 : 1 molar proportion in methanol. Complexes of the general formula [MoO_2LMeOH] were isolated as orange single crystals from the reaction mixture by slow evaporation at room temperature. The complexes are stable in room temperature and are found to be fairly soluble in most of the common organic solvents such as methanol, ethanol, acetonitrile, DMF and DMSO. The low molar solution conductance of the complexes in acetonitrile, indicating the complexes have non-electrolyte behavior.

IR spectra of the aroylhydrazone Schiff bases show bands at about 3230 cm^{-1} for ν(N–H), 3350–3450 cm^{-1} for ν(O–H), and 1650 cm^{-1} for ν(C=O) [18]. The peaks attributed to ν(N–H) and ν(C=O) are absent in the spectra of the complexes as each ligand binds in binegative form losing proton from carbohydrazide group. Strong bands observed at 1605 cm^{-1} for **I** and 1607 cm^{-1} for **II** are attributed to ν(C=N), which are located at lower frequencies as compared to the free aroylhydrazone Schiff bases, *viz.* 1610 cm^{-1} for H_2L^1 and 1613 cm^{-1} for H_2L^2 [19]. The two molybdenum complexes exhibit two characteristic bands at 950 and 861–850 cm^{-1} for asymmetric and symmetric stretching of *cis*-MoO_2^{2+} core, respectively [20, 21].

Electronic spectra of the complexes recorded in acetonitrile solution display strong and medium absorption bands in the regions 390–440 and 290–320 nm. These peaks are assigned as charge transfer transitions of the type N($p\pi$)–Mo($d\pi$) LMCT and O($p\pi$)–Mo($d\pi$) LMCT, respectively [22, 23], as the ligand-based orbitals are either N or O donor types. The slight change of λ_{max} values within each set of peaks may be due to the difference of electron donating capacity of the ligands.

The perspective view of complexes **I** and **II** together with the atom numbering scheme are shown in Fig. 1. The coordination geometry around the molybdenum(VI) atom in the complexes reveals a distorted octahedral environment with NO_5 chromophore. The aroylhydrazone Schiff base behaves as dianionic tridentate ligand binding through the phenolate oxygen, the enolate oxygen and the imine nitrogen, and occupies three positions in the equatorial plane. One oxo group is located *trans* to the imine nitrogen in the equatorial plane. The other oxo group and the methanol oxygen are located at the axial positions. The two terminal oxo groups are hence *cis* to each other and exhibit typical Mo=O double bond distances [24, 25]. The molybdenum is found to be deviated from the mean equatorial plane defined by the four donor atoms by 0.325(1) Å for **I** and 0.330(1) Å for **II**. The Mo–$O_{methanol}$ bond lengths in the complexes are longer than the normal single bond lengths (2.34–2.36 Å against 1.9–2.0 Å). This shows that the methanol molecule is loosely attached to the Mo(VI) center [23]. The remaining Mo–O bond lengths are similar to other molybdenum(VI) complexes [26, 27]. The bond between Mo and the azomethine nitrogen in the complexes are about 2.24 Å which is comparatively longer than the normal Mo–N single bonds. This is due to the *trans* effect generated by the oxo group *trans* to the Mo–N bond [23]. The C(8)–O(2) bond lengths in the complexes are 1.30–1.32 Å, which are closer to single bond length rather than C=O double bond length. However, the shorter length compared to C–O single bond may be attributed to extended electron delocalization in the

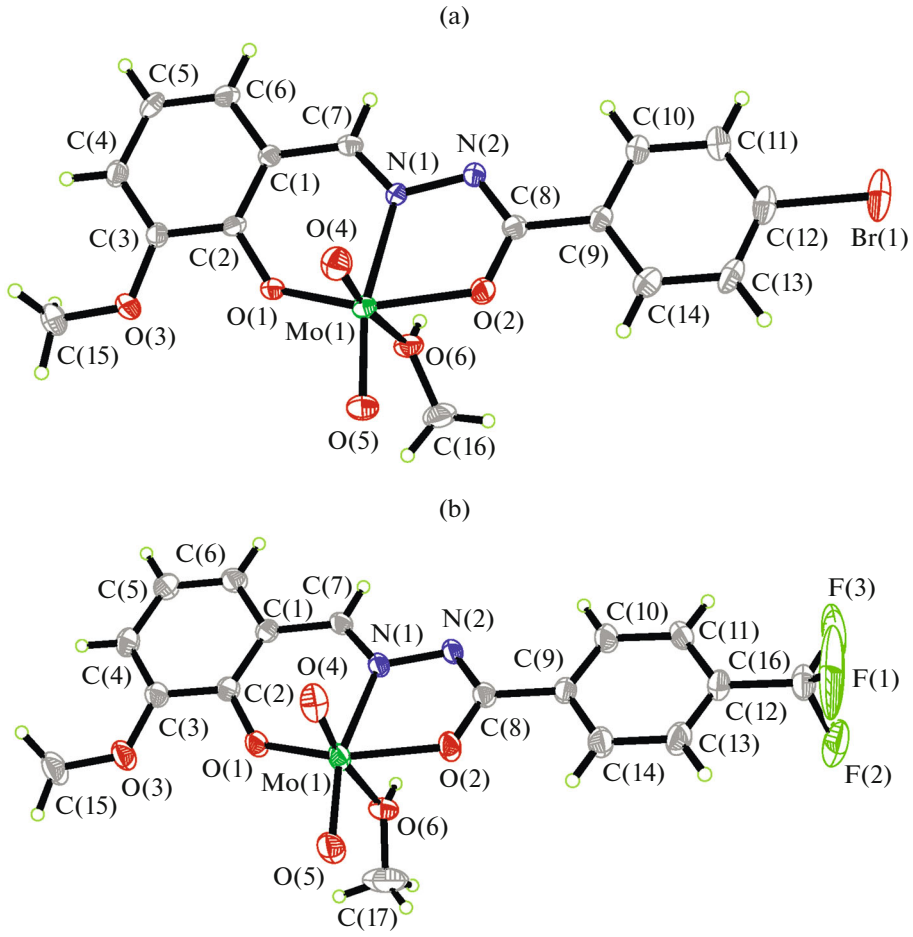

Fig. 1. ORTEP plots (30% probability level) and numbering scheme for **I** (a) and **II** (b).

ligands [23]. Similarly shortening of C(8)–N(2) bond length (1.30–1.31 Å instead of normal 1.38 Å) together with the elongation of N(1)–N(2) bond length also supports the electron cloud delocalization in the ligand system [23]. The aroylhydrazone Schiff base ligand forms a five-membered and a six-membered chelate rings with the Mo center. The five-membered metallacycle ring is thus rather planar, but the six-membered metallacycle ring is clearly distorted. The dihedral angle between the two benzene rings is 5.6(3)° for **I** and 10.5(3)° for **II**. The *trans* angles between the donor atom of the methanol ligand and the oxo atom are 171.72(12)° for **I** and 170.05(11)° for **II**, indicating considerable distortion of the coordination octahedron around the Mo(VI) center.

The crystal packing diagrams of the complexes are quite similar (Fig. 2). The adjacent two complex molecules are linked by two O–H···N hydrogen bonds (**I**: O(6)–H(6) 0.85(1), H(6)···N(2)^{i} 1.94(1), O(6)···N(2)^{i} 2.782(4) Å, O(6)–H(6)···N(2)^{i} 177(5)°; **II**: O(6)–H(6) 0.85(1), H(6)···N(2)^{ii} 1.95(1), O(6)···N(2)^{ii} 2.791(4) Å, O(6)–H(6)···N(2)^{ii} 170(5)°; symmetry

Table 3. Catalytic results for the cyclooctene epoxidation by aqueous TBHP[a]

Complex	Conversion, %[b]	Selectivity, %[c]	TOF, h^{-1} [d]	TON[e]
I	92	57	387	372
II	86	52	340	355

[a] Reaction conditions: time, 5 h; temperature, 80°C. Molybdenum complex : cyclooctene : TBHP molar ratio: 0.25 : 100 : 200.
[b] For cyclooctene, calculated after 5 h.
[c] Formed epoxide per converted olefin after 5 h.
[d] *n*(Cyclooctene transformed)/*n*(catalyst)/time at 20 min.
[e] *n*(Cyclooctene transformed)/*n*(catalyst) at 5 h.

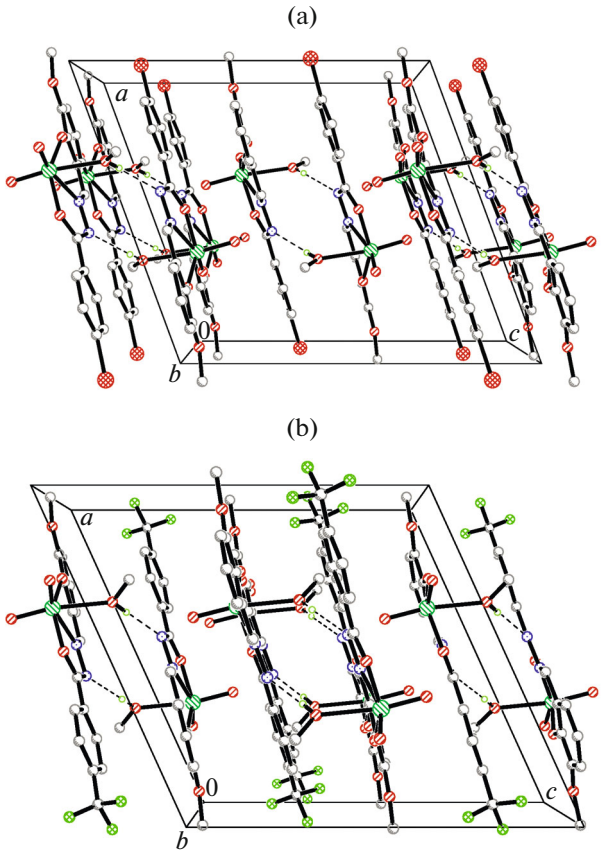

Fig. 2. Hydrogen bond (dashed lines) linked structure of **I** (a) and **II** (b), viewed down the *b* axis.

codes: [i] $1-x, 2-y, -z$; [ii] $1-x, 1-y, -z$), to form dimer.

After addition of aqueous TBHP at 80°C, the molybdenum complexes dissolve completely in the organic phase. The aqueous phase of the complexes was colorless and the organic one yellowish, indicating that the catalyst is mainly confined in the organic phase. TBHP is mainly transferred into the organic phase under those conditions, and for that reason the reactant and products in the organic layer were analyzed. Cyclooctene and cyclooctene oxide are not significantly soluble in water, therefore the determination of the epoxide selectivity (epoxide formation/cyclooctene conversion) is expected to be accurate. The obtained results are given in Table 3. For the cyclooctene epoxidation by using aqueous TBHP with no extra addition of organic solvents, the present study shows effective activity. Kinetic profiles of the molybdenum complexes as catalysts are presented in Fig. 3. No induction time was observed. The cyclooctene conversion for the molybdenum complexes is high after 5 h, *viz*. 92% for **I** and 86% for **II**.

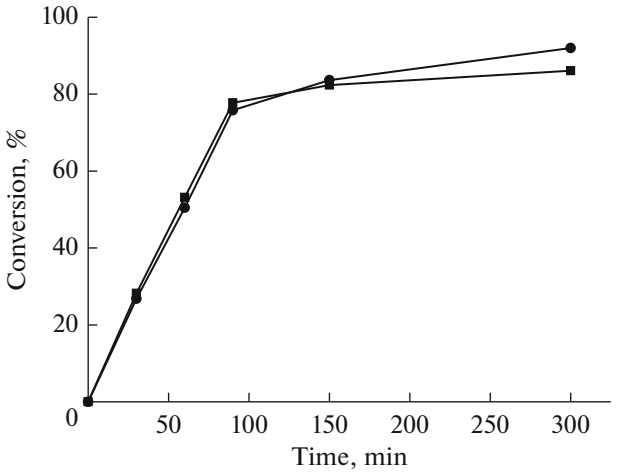

Fig. 3. Kinetic monitoring of *cis*-cyclooctene epoxidation with TBHP–H_2O in the presence of the molybdenum complexes **I** (●), **II** (■).

Possible mechanistic consideration involves coordination of TBHP as a neutral molecule with the hydrogen bond O–H···O (Scheme 2). Even though high conversion of cyclooctene is observed, selectivity towards cyclooctene oxide is not high, with 52% for **I** and 57% for **II**.

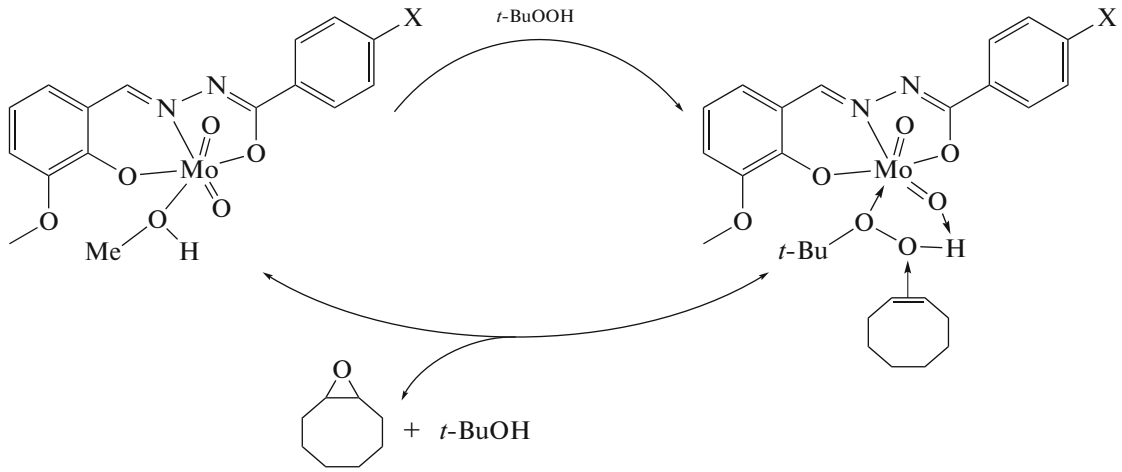

Scheme 2.

In summary, the present paper reports a very common but facile way to synthesize two new Mo(VI) complexes with aroylhydrazone Schiff bases. In the complexes, the aroylhydrazone Schiff base ligands differ only in the terminal substitute groups of the phenyl rings, *viz.* Br for **I** and CF_3 for **II**. The complexes are efficient catalysts for the epoxidation of cyclooctene.

ACKNOWLEDGMENTS

This work was supported by the Collaborative Innovation Plan of Hubei Province for Key Technology of Eco-Ramie Industry.

REFERENCES

1. Heffern, M.C., Reichova, V., Coomes, J.L., et al., *Inorg. Chem.*, 2015, vol. 54, no. 18, p. 9066.
2. Meghdadi, S., Amirnasr, M., Majedi, M., et al., *Inorg. Chim. Acta*, 2015, vol. 437, p. 64.
3. Qu, D., Niu, F., Zhao, X., et al., *Bioorg. Med. Chem.*, 2015, vol. 23, no. 9, p. 1944.
4. Zafar, H., Ahmad, A., Khan, A.U., et al., *J. Mol. Struct.*, 2015, vol. 1097, p. 129.
5. Zhao, X., Chen, X., Li, J., et al., *Polyhedron*, 2015, vol. 97, p. 268.
6. Mohamed, R.G., Elantabli, F.M., Helal, N.H., et al., *Synth. React. Inorg. Met.-Org. Nano-Met. Chem.*, 2015, vol. 45, no. 12, p. 1839.
7. Oliveira, T.S.M., Gomes, A.C., Lopes, A.D., et al., *Dalton Trans.*, 2015, vol. 44, no. 31, p. 14139.
8. Koellner, C.A., Piro, N.A., Kassel, W.S., et al., *Inorg. Chem.*, 2015, vol. 54, no. 15, p. 7139.
9. Alemohammad, T., Safari, N., Rayati, S., et al., *Inorg. Chim. Acta*, 2015, vol. 434, p. 198.
10. Bagherzadeh, M., Ghanbarpour, A., and Khavasi, H.R., *Catal. Commun.*, 2015, vol. 65, p. 72.
11. Liu, H.Y., Zang, L.Q., and Lv, J.L., *Russ. J. Coord. Chem.*, 2015, vol. 41, no. 7, p. 451. doi 10.1134/S1070328415070052
12. Morales-delaRosa, S., Campos-Martin, J.M., Terreros, P., et al., *Top. Catal.*, 2015, vol. 58, nos. 4–6, p. 325.
13. Baskaran, T., Kumaravel, R., Christopher, J., et al., *New J. Chem.*, 2015, vol. 39, no. 5, p. 3758.
14. Amir, M. and Shikha, K., *Eur. J. Med. Chem.*, 2004, vol. 39, no. 6, p. 535.
15. Chen, G.J.J., McDonald, J.W., and Newton, W.E., *Inorg. Chem.*, 1976, vol. 15, no. 11, p. 2612.
16. Sheldrick, G.M., *SADABS, Siemens Analytical X-ray Instrument Division*, Madison, 1995.
17. Sheldrick, G.M., *SHELXS-97, Program for Solution of Crystal Structures*, Göttingen: Univ. of Göttingen, 1997.
18. Ye, Y.-T., Niu, F., Sun, Y., et al., *Chin. J. Inorg. Chem.*, 2015, vol. 31, no. 5, p. 1019.
19. You, Z.-L., Xian, D.-M., and Zhang, M., *CrystEngComm*, 2012, vol. 14, no. 21, p. 7133.
20. Lal, R.A., Chakrabarty, M., Choudhury, S., et al., *J. Coord. Chem.*, 2010, vol. 63, no. 1, p. 163.
21. Glowiak, T., Jerzykiewicz, L., Sobczak, J.M., et al., *Inorg. Chim. Acta*, 2003, vol. 356, p. 387.
22. Hahn, R. and Kusthardt, U., *Inorg. Chim. Acta*, 1993, vol. 210, no. 2, p. 177.
23. Gupta, S., Barik, A.K., Pal, S., et al., *Polyhedron*, 2007, vol. 26, no. 1, p. 133.
24. Bagherzadeh, M., Amini, M., Parastar, H., et al., *Inorg. Chem. Commun.*, 2012, vol. 20, p. 86.
25. Dinda, R., Sengupta, P., Ghosh, S., et al., *Dalton Trans.*, 2002, no. 23, p. 4434.
26. Dinda, R., Ghosh, S., Falvello, L.R., et al., *Polyhedron*, 2006, vol. 25, no. 12, p. 2375.
27. Vrdoljak, V., Prugovecki, B., Matkovic-Calogovic, D., et al., *Cryst. Growth Des.*, 2011, vol. 11, no. 4, p. 1244.